Title
Digitally fabricated multi-modal wireless sensing using a combination of printed sensors and transistors with silicon components

Journal
Flexible and Printed Electronics, 2(3)

ISSN
2058-8585

Authors
Whiting, GL
Schwartz, DE
Ng, TN
et al.

Publication Date
2017-09-01

DOI
10.1088/2058-8585/aa7c0f

Peer reviewed

Flexible and Printed Electronics

PAPER

Digitally fabricated multi-modal wireless sensing using a combination of printed sensors and transistors with silicon components

To cite this article: G L Whiting *et al* 2017 *Flex. Print. Electron.* **2** 034002

Flexible and Printed Electronics

CrossMark

RECEIVED
7 March 2017

REVISED
19 June 2017

ACCEPTED FOR PUBLICATION
27 June 2017

PUBLISHED
23 August 2017

PAPER

Digitally fabricated multi-modal wireless sensing using a combination of printed sensors and transistors with silicon components

G L Whiting[1,5,6], D E Schwartz[1,6], T N Ng[1,7], B S Krusor[1], R Krivacic[1], A Pierre[2], A C Arias[2], M Härting[3], D van Buren[4] and K L Short[4]

[1] Palo Alto Research Center, 3333 Coyote Hill Road, Palo Alto, CA 94304, United States of America
[2] University of California Berkeley, Department of Electrical Engineering and Computer Sciences, Cory Hall, Berkeley, CA 94720, United States of America
[3] University of Cape Town, NanoSciences Innovation Centre, Department of Physics, Rondebosch 7701, Cape Town, South Africa
[4] Jet Propulsion Laboratory, 4800 Oak Grove Drive, Pasadena, CA 91109, United States of America
[5] Current address: University of Colorado Boulder, Department of Mechanical Engineering, 1111 Engineering Drive, UCB 427, Boulder, CO 80309, United States of America
[6] Authors to whom any correspondence should be addressed.
[7] Current address: University of California San Diego, Department of Electrical Engineering, 9500 Gillman Drive, La Jolla, CA 92093, United States of America.

E-mail: gregory.whiting@colorado.edu and david.schwartz@parc.com

Keywords: printed electronics, flexible electronics, organic semiconductors, photovoltaic, printed sensors, wireless system, systems integration

Abstract

Printing is a promising manufacturing approach for the fabrication of flexible, large-area, custom sensor systems for applications such as wearable electronics and sensor labels. While printed examples of many physical and chemical sensors have been demonstrated, functionality useful for stand-alone systems such as high-resolution analog-to-digital conversion and wireless communication to address these sensors is not currently available in circuits printed entirely from solution. In order to retain the benefits of print manufacturing without sacrificing performance, a hybrid approach can be followed where printed and pre-fabricated devices are used together. In this report a mostly-printed wireless light and temperature sensor system that operates at 3.6 V and reports light and temperature readings wirelessly with a sensitivity of 0.7 °C and 2.5 μW cm^{-2} at 500 nm respectively is demonstrated. The number of printed components was maximized and off-the-shelf microfabricated devices were only introduced where functionality is not currently achievable through printing. Onto a flexible polyester substrate, print processes were used to fabricate the bulk-heterojunction photodiode, thermistor, low-voltage operation multiplexing transistors, antenna, passives and interconnects, and silicon ICs are used for signal processing, memory and wireless communication. The printed components (sensors and transistors) were specifically developed to facilitate electrical integration into the hybrid system.

Introduction

Electronic systems printed from solution provide a significant number of benefits including large-area processing, facile customization, low cost and, typically, low mass and mechanical flexibility. Using printing techniques [1], a broad range of sensors [2, 3], actuators [4, 5], circuits [6–8], power sources [9, 10], data storage [11, 12], and communication electronics [13, 14] have been developed allowing complex printed systems to be designed and demonstrated. However, due to the relatively large minimum feature sizes attainable with most printing techniques, typically tens of microns, circuit performance is constrained when compared with microfabricated single crystal silicon complementary metal-oxide-semiconductor (Si-CMOS) devices. Certain complex functionalities, such as high-resolution analog-to-digital conversion, radio-frequency (RF) communication and complex logic, are particularly difficult to achieve reliably with printed circuits. High-performance

printed sensors, however, can be readily fabricated through solution-based printing without area constraints. In order to best utilize such printed sensors in complete systems, complex electronic functionality to process and transmit the sensor state is essential.

To provide for more capable mechanically flexible printed electronic systems, a mixture of printed and Si-CMOS integrated circuit (IC) components are combined in this report. This hybrid approach enables high-performance systems to be realized while retaining the customizability, sparse large-area coverage and small but versatile materials set available when using print-based prototyping. Mechanical flexibility can also be readily retained even for brittle inorganic materials, as long as such components are small and/or thin and are isolated on the pliable polymeric substrates. Flexible electronics have previously been demonstrated using thin high-performance electronic devices and materials including off-the-shelf microelectronic components [15], and are relevant for application areas including wearable electronics, sensor labels, and energy harvesting amongst others.

The divergent electronic properties of printed electronic circuits and sensors and off-the-shelf Si-CMOS components presents a challenge for their integration. For example, due to the relatively thick dielectric layers and low mobility organic materials used to fabricate printed circuits, the operating voltages are typically on the order of tens of Volts and the operating resistances of these devices are often in the MΩ range [16]. Such values are in many cases incompatible with microfabricated devices that typically operate below 5 V and require lower impedance direct inputs than those provided by printed sensors and circuits. These concerns can be addressed by adding additional components, such as charge pumps and operational amplifiers, but this creates additional complexity, limiting the applicability and ease of fabrication of these systems.

Experimental section

Printed sensors

Bulk-heterojunction photodiodes consist of a layer of blade-coated PEDOT:PSS as the transparent electrode, followed by a blade-coated PTB7:$PC_{71}BM$ active layer using 3 vol.% 1,8-diiodooctane in chlorobenzene, and a thermally evaporated aluminum cathode. To complete the devices they were encapsulated using a UV-curable epoxy.

The temperature sensor was fabricated by screen printing of an ink of milled silicon particles for the thermistor and a carbon-loaded ink for the resistor onto 100 μm polyethylene terephthalate (PET) substrates. Interdigitated electrodes, interconnects and the external contacts were first laid down using a solvent-based silver ink (Dupont 5000). After completion the device, except for the contact pads, was overprinted with a screen printable encapsulant (Dupont 5036) for protection.

Printed multiplexing transistors

Top-gate multiplexor organic thin-film transistors (TFTs) were fabricated following a similar method as previously reported [29, 30]. Onto polyethylene naphthalate (PEN) substrates source-drain electrodes were ink-jet printed using a piezoelectric head from a silver nanoparticle dispersion (35 μm S–D gap). To form the injection layer, the electrodes were submerged in a solution of F_4TCNQ (0.5% in o-dichlorobenzene) for ~2 min and the substrate is then rinsed with dichloromethane and dried. A *p*-type organic semiconductor (OSC) (Flexink 82) was then ink-jet printed over the source/drain electrodes. The bilayer dielectric was spin-coated over the semiconductor using a thin layer (40 nm) of a perfluoropolymer (Teflon AF), overcoated with a thick (0.7 μm) P(VDF-TrFE-CTFE) terpolymer layer. The gate electrode was then ink-jet printed using a silver nanoparticle dispersion.

Passive components

The static resistor (MΩ) for the photodiode bridge was ink-jet printed from a carbon nanoparticle based ink onto PEN, pull-up resistors (kΩ) were ink-jet printed from a silver nanoparticle dispersion onto PEN, the RF antenna was extrusion printed from an auger head using a thick silver particle loaded ink (DuPont 5028), and the antenna capacitor was formed from ink-jet printed silver electrodes and a spin-coated perfluoropolymer/terpolymer dielectric.

System fabrication

The interconnect layout was extrusion printed using a Nordson auger device onto a master PEN substrate (DuPont Teijin, 125 μm thick) from a silver particle loaded ink (DuPont 5028). Cross-overs were formed using kapton tape for isolation and overprinted using extrusion of the silver particle loaded ink. Programming of the chips was carried out using a socket on a separate printed circuit board. Separate printed photosensors, temperature sensors, multiplexing transistors, pull-up resistors, divider resistor, capacitor and microelectronic components (PIC: Microchip PIC16 (L)F1503, RF IC: ST Microelectronics M24LR64-R) were manually mounted to one side of the master substrate, affixed with a non-conductive two-part epoxy adhesive (Henkel Corp. Loctite Quickset) and interconnected using the 5028 ink. The antenna was affixed to the reverse side of the master substrate and interconnected into the system through holes punched in the PEN filled with silver ink.

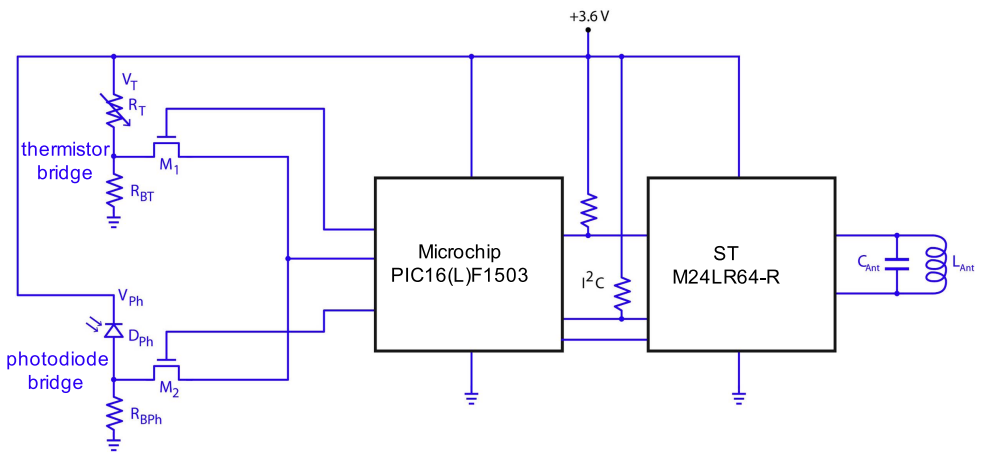

Figure 1. Schematic diagram showing the layout of the sensor system. Blue color indicates printed components, black indicates pre-fabricated components.

Results and discussion

In this report we demonstrate a hybrid printed sensing system for wireless monitoring of temperature and irradiance. Figure 1 shows a schematic layout for this device. Temperature and light sensors, multiplexing FETs, resistors, capacitors, the antenna and interconnects were printed from solution-based inks using a variety of techniques and packaged off-the-shelf components were used for analog-to-digital conversion, and near-field RF communication.

This design and material set was selected to provide the required functionality with a minimal number of components. Single resistors are minimally sufficient for converting resistive or current sensor signals to voltages for readout by the microcrontroller analog-to-digital converter. More accurate bridge circuits require matched resistor values, which are challenging to produce with printing, and differential readout circuits. A printed two-TFT multiplexor is used to array the printed sensors and is addressed directly by the digital outputs on the microcontroller, making it easily extendible to include more sensors in future versions without the need for a separate multiplexing chip.

The microcontroller and communications chip do not require any external passive resistors, capacitors, or crystals, except for the two pull-up resistors on the integrated circuit communication path. The communications chip has built-in 64-kbit EEPROM memory, and operates at RFID-standard 13.56 MHz with a printed coil antenna and printed single filter capacitor.

Bulk heterojunction photodiodes based on a polymer/fullerene blend were used for light sensing (figures 2(A)–(C)). Devices were fabricated on a polyethylene naphthalate (PEN) substrate using a combination of surface energy-patterning and doctor blading reported previously [17, 18]. The dark current of the device is below 10^{-8} A cm^{-2} under the operation regime as shown in figure 2(A) with an external quantum efficiency of approximately 20% and 55% at short circuit and −2 V bias, respectively, as shown in figure 2(B). This yields specific detectivity ranging from 3.7×10^{12}–5.6×10^{12} Jones throughout the visible spectrum, which is comparable to most silicon photodiodes. The dynamic range of the photodiode in figure 2(C) shows a nonlinear response most likely as a result of either space-charge limited current or bimolecular recombination [19].

Temperature sensors were screen printed onto PET substrates and are composed of a printed silicon thermistor and a printed carbon resistor connected together in series to form a voltage divider. The thermistor body was printed using a water-based silicon nanoparticle ink containing particles produced by milling of bulk silicon [20] which have no appreciable surface oxide [21]. In the printed layer, the silicon nanoparticles form a hierarchical network of clusters [22]. Thermistor characteristics arise from charge transfer between these clusters of nanoparticles with well-defined activation energies. The resistor was printed with a solvent-based carbon particle ink, blended to match the resistance of the thermistor in the temperature range of interest. The resistances of both components were targeted to be in the MΩ range using a combination of the respective ink compositions and the internal electrode geometry. Figures 2(D) and (E) show the performance of the thermistor and voltage divider respectively. The thermistor is a negative temperature coefficient device providing a decrease in resistance as the temperature is increased with an activation energy of 0.2 eV. When combined with the printed carbon resistor (which has a weak positive temperature coefficient) in a resistive divider configuration, a roughly linear decrease in output voltage is observed over the tested temperature range (20 °C–70 °C).

To avoid the need for multiple voltage rails, it is desirable to operate the multiplexing circuits at the supply voltage for the microcontroller (3.6 V). Printed

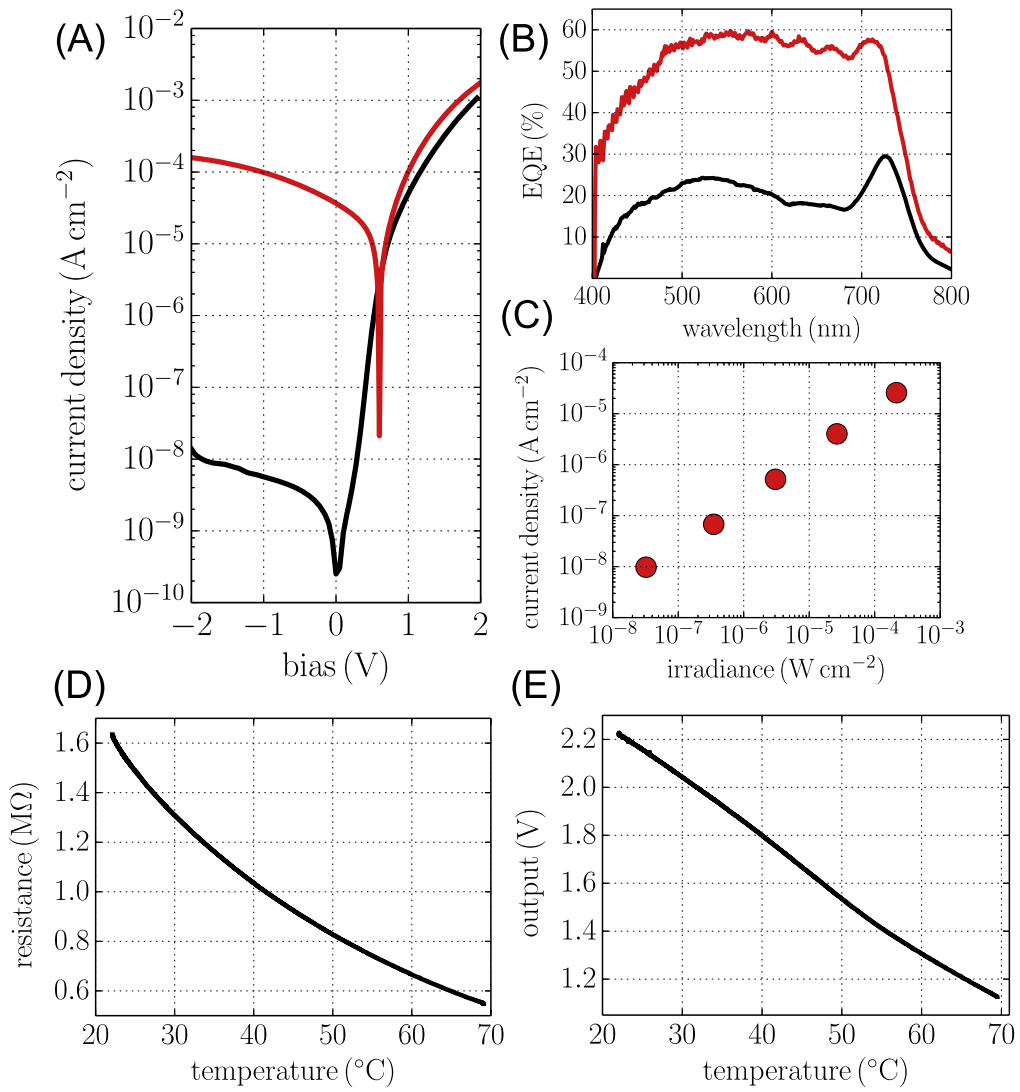

Figure 2. Characteristics of light and temperature sensors. (A) JV data for the photosensor under 557 μW cm^{-2} at 640 nm illumination (red line) and in the dark (black line). (B) Photosensor spectral response at −2 V (red line) and 0 V (black line). (C) Photosensor dynamic response at 0 V. (D) Thermistor response (1 V supply). (E) Resistive divider output of thermistor and carbon-based resistor (3.6 V supply).

organic FETs often operate at higher voltages. The print process typically leads to topographically rough layers that require high dielectric thickness (>0.5 μm) to provide reliable isolation between the semiconductor and gate electrode in an FET. Furthermore, low-k dielectrics are usually needed at the semiconductor/dielectric interface in OSC based FETs in order to reduce dipolar disorder and improve charge transport mobility [23]. This combination of high thickness and low-k leads to low areal capacitance, requiring high voltages (typically tens of volts) to provide the necessary field to operate the devices.

To overcome this issue various approaches have previously been applied to increase the capacitance of the dielectric in organic FETs. By increasing either the dielectric constant or reducing the thickness of the dielectric, the capacitance can be improved. Reduction of the thickness down to a few nanometers has previously been described and has provided low-voltage operation for organic TFTs [24], however this approach can be problematic for devices processed using printing over large areas, where defects either increase gate leakage or cause shorts, decreasing yield. High-k dielectrics have also been used and have proved effective but are often not compatible with top-gate device structures [25]. Another interesting class of high-k dielectrics that can be solution processed and have been incorporated successfully into low-voltage printed organic FETs are ionic liquids or gels [26], which can be deposited in relatively thick layers (>1 μm—reducing leakage and improving yield) while also providing useful transistor operation below 1 V, but may require more complex packaging than a completely solid-state dielectric.

Here, a thick relaxor terpolymer (poly(vinylidene difluoride-co-trifluoroethylene-co-chlorotrifluoroethylene)) [P(VDF-TrFE-CTFE)] with a k of ~40 is used as the gate dielectric. The inclusion of the

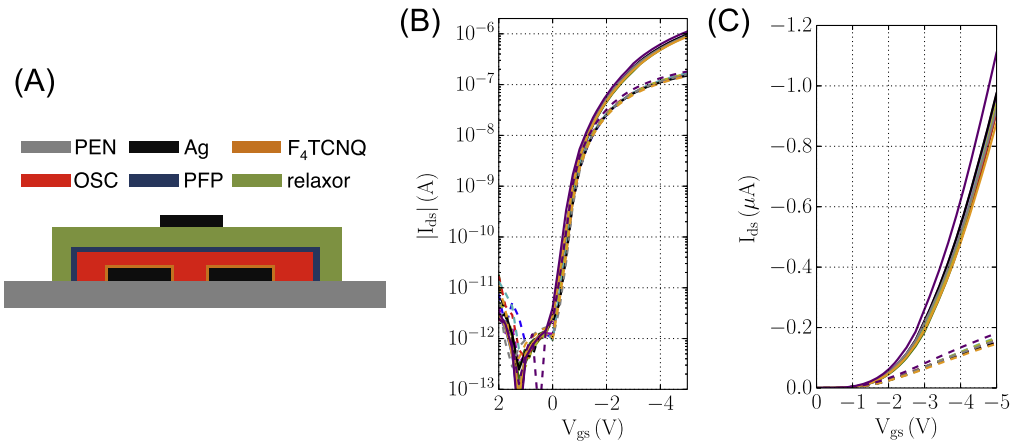

Figure 3. Field-effect transistors for signal multiplexing (A) Printed TFT structure (OSC—organic semiconductor, PFP—perfluoropolymer). (B) Semilog plot of transfer characteristics for ten printed FETs taken at $V_{ds} = -0.5$ V (dotted lines) and $V_{ds} = 5$ V (solid lines) ($W = 0.68$ mm, $L = 37$ μm). (C) Linear plot of transfer characteristics for the same ten printed FETs taken at $V_{ds} = -0.5$ V (dotted lines) and $V_{ds} = -5$ V (solid lines) ($W = 0.68$ mm, $L = 37$ μm).

CTFE unit disrupts the organization of the polymer, suppressing the ferroelectric properties typically associated with PVDF and its copolymers [27]. In order to provide a low energy semiconductor-dielectric interface and to protect the semiconductor from further solution processing in this top-gate device a thin (~40 nm) spin-coated perfluoropolymer layer (Teflon AF) is inserted between the semiconductor and the dielectric, forming a bilayer. This fluoropolymer bilayer dielectric shows a number of useful benefits: it provides a low energy interface to improve charge transport mobility, uses an orthogonal perfluorosolvent for processing on top of the semiconductor, is relatively thick (~0.7 μm) to reduce gate leakage, prevent shorting and improve yield, presents a top surface with suitable surface energy for printing the gate contact and provides a relatively high gate capacitance (24 nF cm^{-2}) to allow operation at the 3.6 V supply voltage.

Characteristics for the printed multiplexing transistors fabricated using this bilayer dielectric and used for the sensor system are shown in figure 3. These top-gate devices are based on a *p*-type polymeric OSC (Flexink 82) which is ink-jet printed onto a PEN substrate with 2,3,5,6-tetrafluoro-7,7,8, 8-tetracyanoquinodimethane (F_4TCNQ) [28] modified ink-jet printed silver nanoparticle source and drain contacts. The bilayer fluoropolymer dielectric is then coated on top and a silver nanoparticle gate electrode is ink-jet printed to complete the device. As shown in figure 3, these devices are clearly in an 'on' state at 3.6 V and an 'off' state at 0 V giving an on-off ratio of $>10^5$ between these operating points, indicating their suitability as multiplexing switches for this system. Charge transport mobility and threshold voltage (extracted from a linear fit to the square root of the transfer curves in the saturation regime) for these printed transistors is 0.30 ± 0.02 cm^2 V^{-1} s^{-1} and -1.2 ± 0.1 V respectively.

Fabrication of the complete system was carried out through assembly of the separate printed components onto a master substrate patterned with interconnect. First the interconnect layout was extrusion printed onto a 125 μm thick PEN master substrate (DuPont Teijin) using a viscous silver particle ink (DuPont 5028) from an Nordson auger-type dispenser. This approach provides thick, robust, low-resistance traces that can readily be connected to the various assembled components. This ink was also used to form a six-turn planar coil antenna with a peak resonance frequency of 13.56 MHz and a DC resistance of ~25 Ω. The commercially available PIC microcontroller (Microchip PIC16(L)F1503) and RF chip (ST Microelectronics M24LR64-R) were programmed and then mounted to the substrate using a non-conductive two-part epoxy adhesive, and electrically connected to the system using the silver particle ink. This provided a robust mechanical and electrical interconnection that could be repeatedly flexed without noticeable damage down to a radius of curvature >1 cm. The same attachment strategy was then used to mount the various printed components: the temperature sensor divider, the photodiode and associated divider resistor, the two multiplexing field-effect transistors (FETs) (one for each sensor), the antenna and associated capacitor and two pull-up resistors. Table 1 provides a description of each of the components used in the hybrid system, and figure 4(A) shows an optical image of the completed sensor foil. Out of caution, deliberate testing of the mechanical flexibility of the completed system was not carried out, however, it was noted that minimal repeated flexing as was experienced through regular handling (bend radius of roughly >10 cm) did not cause any noticeable damage to either the mechanical or electrical properties of the device.

The sensor system is powered from an external 3.6 V DC source and operates automatically and continuously (the low power and voltage requirements

Table 1. Description of the various components of the sensor system.

Component	Purpose	Fabrication method	Active material
	Active components		
Field effect transistor	Sensor signal multiplexing	Ink-jet printed	Organics
Photosensor	Light sensing	Blade coated	Organics
Thermistor	Temperature sensing	Screen printed	Si nanoparticles
PIC microcontroller	A2D conversion, data processing	Pre-fabricated	Si CMOS
RF chip	Wireless communication, memory	Pre-fabricated	Si CMOS
	Passive components		
Capacitor	Antenna impedance matching	Ink-jet printed	Organics
kΩ resistor	Pull-up resistors	Ink-jet printed	Ag nanoparticles
MΩ resistor	Sensor signal conversion	Ink-jet and screen printed	C particles
Antenna	Wireless communication	Extruded	Ag particles
	Others		
Conductive tracks	Electrical interconnection	Extruded	Ag particles

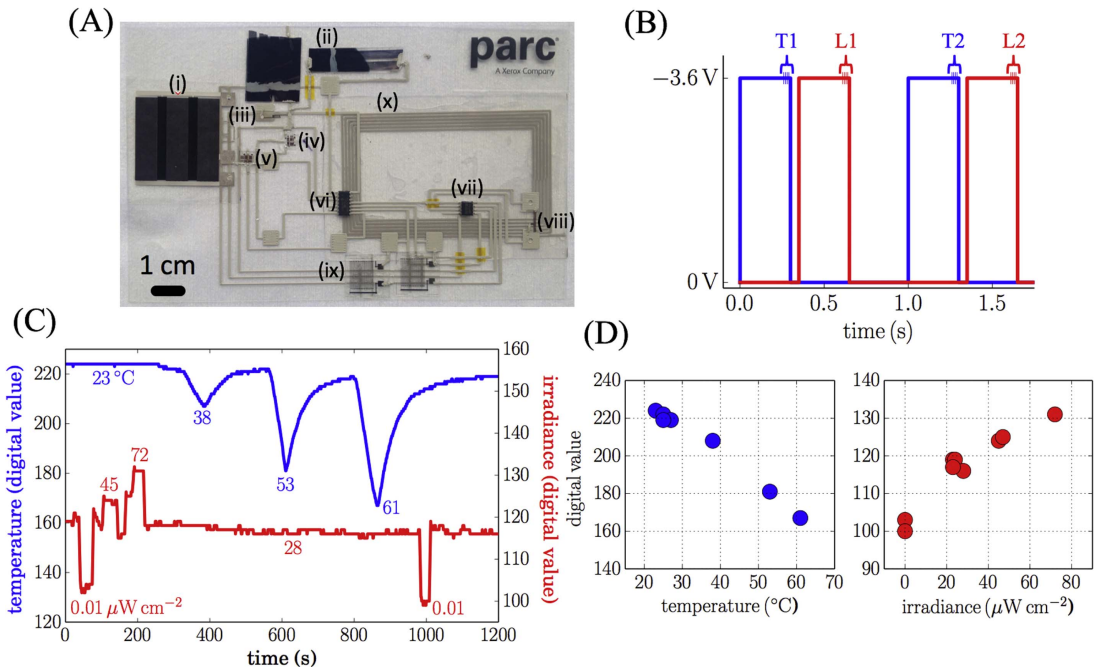

Figure 4. Complete sensor system. (A) Optical image of device with the various components annotated (i) thermistor and static resistor for temperature sensor bridge (R_T and R_{BT}) (ii) photodiode (D_{Ph}) (iii) static resistor for photodiode bridge (R_{BPh}) (iv) photodiode multiplexing TFT (M_2) (v) thermistor multiplexing TFT (M_1) (vi) PIC (vii) RF IC (viii) antenna capacitor (C_{ant}) (ix) pull-up resistors, antenna. (B) Gating signals for the multiplexing TFTs for the temperature sensor (blue line) and the photosensor (red line) T1 & T2 indicate the 1st and 2nd measurements taken from the temperature sensor and L1 & L2 indicate the 1st and 2nd measurements taken from the photosensor. (C) Irradiance (500 nm light, red line) and temperature (blue line) data taken from sensor system. (D) Calibration data for temperature (blue points) and irradiance (500 nm light, red points).

would allow future versions to be powered from thin-film printed electrochemical cells). The two enable TFTs forming the multiplexer are alternately turned on for 300 ms with application of 3.6 V from a digital output pin from the PIC. During this period, four sequential samples are taken. The values are averaged and stored in the memory of the RF chip. After the measurement is complete, the data is read via a command from a remote reader unit. An illustration of the gating signals is shown in figure 4(B).

The system was tested and calibrated through exposure to heat (hot air gun) and light (broadband incandescent source though a 500 nm filter), of various levels over the course of about 20 min. After the experiment was complete the data were read off wirelessly (a maximum reading distance of ~7 cm was observed) from the printed system using a short range RF reader (ISO15693-ST Microelectronics DEMO-KIT-M24LR-A). Data from a representative experiment displayed in figure 4(C) show that the system operates as expected with minimal cross-talk between the sensors. Calibration curves are shown in figure 4(D). For the irradiance and temperature range, the sensor response is roughly linear (particularly for

the temperature sensor), and the temperature and light sensor have a sensitivity of ~0.7 °C and 2.5 μW cm^{-2} at 500 nm, respectively.

Conclusion

In summary, a sensor system has been demonstrated to measure both temperature and irradiance using wireless readout by following a hybrid approach that integrates printed electronic devices where possible with pre-fabricated Si-CMOS components where necessary. The printed sensors were multiplexed using low-voltage printed TFTs, providing a simple circuit that minimizes the number of inputs to the silicon chip and provides an approach to expanding the number of sensors that can be addressed by a single chip without the need for additional pre-fabricated components. Sensor signal processing was carried out using a silicon microcontroller and the sensor data was stored and wirelessly communicated using an RF chip and printed antenna. This hybrid approach enables digital print fabrication of a sensor foil with improved performance when compared with an electronic system prepared entirely from solution-based inks, by combining the computing power of Si-CMOS ICs with the advantages of printed components to enable flexible form factor, on-location print manufacturability, and facile customization.

Acknowledgments

We thank Sivkheng Kor and Alexander Tugaov for their valuable assistance with device fabrication and RF design. This work was supported by a grant from the NASA Innovative Advanced Concepts (NIAC) program (grant number 12-12NIAC II-0017). This work was supported in part by the National Science Foundation under Cooperative Agreement No. EEC-1160494 and by the NSF Graduate Fellowship Research Program under Grant No. DGE-1106400. This work was also supported in part by Systems on Nanoscale Information fabriCs (SONIC), one of the six SRC STARnet Centers, sponsored by MARCO and DARPA.

References

[1] Arias A C, MacKenzie J D, McCulloch I, Rivnay J and Salleo A 2010 *Chem. Rev.* **110** 3–24
[2] Hammock M L, Chortos A, Tee B C-K, Tok J B-H and Bao Z 2013 *Adv. Mater.* **25** 5997–6038
[3] Mabeck J T and Malliaras G G 2006 *Anal. Bioanal. Chem.* **384** 343–53
[4] Fukuda K *et al* 2011 *Adv. Funct. Mater.* **21** 4019–27
[5] Kwon K K and Ng T N 2014 *Org. Electron.* **15** 294–8
[6] Marien H, Steyaert M S J, Van Veenendaal E and Heremans P L P L 2012 *IEEE Solid-State Circuits Mag.* **4** 43–9
[7] Sekitani T and Someya T 2010 *Adv. Mater.* **22** 2228–46
[8] Ng T N *et al* 2012 *Sci. Rep.* **2** 585
[9] Gaikwad A M, Steingart D A, Ng T N, Schwartz D E and Whiting G L 2013 *Appl. Phys. Lett.* **102** 233302
[10] Gaikwad A M, Whiting G L, Steingart D A and Arias A C 2011 *Adv. Mater.* **23** 3251–5
[11] Naber R C G, Asadi K, Blom P W M, de Leeuw D M and de Boer B 2010 *Adv. Mater.* **22** 933–45
[12] Baeg K-J, Khim D, Kim J, Yang B-D, Kang M, Jung S-W, You I-K, Kim D-Y and Noh Y-Y 2012 *Adv. Funct. Mater.* **22** 2915–26
[13] Jung M *et al* 2010 *IEEE Trans. Electron Devices* **57** 571–80
[14] Cantatore E, Geuns T C T, Gelinck G H, van Veenendaal G H E, Gruijthuijsen A F A, Schrijnemakers L, Drews S and de Leeuw D M 2007 *IEEE J. Solid-State Circuits* **42** 84–92
[15] Xu S *et al* 2014 *Science* **344** 70–4
[16] Street R A 2009 *Adv. Mater.* **21** 2007–22
[17] Pierre A, Sadeghi M, Payne M M, Facchetti A, Anthony A J E and Arias A C 2014 *Adv. Mater.* **26** 5722–7
[18] Lochner C M, Khan Y, Pierre A and Arias A C 2014 *Nat. Comm.* **5** 5745
[19] Baeg K-J, Binda M, Natali D, Caironi M and Noh Y-Y 2013 *Adv. Mater.* **25** 4267–95
[20] Britton D T and Härting M 2006 *Pure Appl. Chem.* **78** 1723–39
[21] Härting M, Zhang J, Gamota D R and Britton D T 2009 *Appl. Phys. Lett.* **94** 193509
[22] Jonah E O, Britton D T, Beaucage P, Rai D K, Beaucage G, Magunje B, Ilavsky J, Scriba M R and Härting M 2012 *J. Nanopart. Res.* **14** 1249
[23] Veres J, Ogier S, Lloyd S G and de Leeuw D 2004 *Chem. Mater.* **16** 4543–55
[24] Halik M, Klauk H, Zschieschang U, Maisch S, Effenberger F, Dehm C, Schu M, Brunnbauer M and Stellacci F 2004 *Nature* **431** 963–6
[25] Park Y M, Desai A, Salleo A and Jimison L 2013 *Chem. Mater.* **25** 2571–9
[26] Kim S H, Hong K, Xie W, Lee K H, Zhang S, Lodge T P and Frisbie C D 2013 *Adv. Mater.* **25** 1822–46
[27] Chu B, Zhou X, Ren K, Neese B, Lin M, Qang Q, Bauer F and Zhang Q M A 2006 *Science* **313** 334–6
[28] Whiting G L and Arias A C 2009 *Appl. Phys. Lett.* **95** 253302
[29] Ng T N, Schwartz D E, Mei P, Krusor B, Kor S and Veres J 2015 *Sci. Rep.* **5** 13457
[30] Mei P, Ng T N, Lujan R A, Schwartz D E, Kor S, Krusor B S and Veres J 2014 *Appl. Phys. Lett.* **105** 123301